Geochemical Perspectives Letters

Neoarchean marine chemical sediments as archives of Hadean silicate differentiation

A.N. Wainwright[1,2*], V. Debaille[1], J.E. Hoffmann[3], S. Viehmann[4], M. Bau[5]

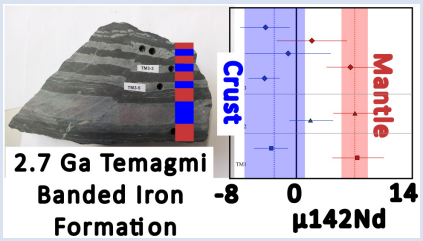

Planetary differentiation had a profound influence on the geochemical signature of the Earth's silicate reservoirs. Some of the early created complementary reservoirs dissipated with time (*e.g.*, Bennett *et al.*, 2007) and only remnants can be observed. Here, we apply the short lived isotopic system ^{146}Sm-^{142}Nd to an alternative archive—marine chemical sediments—and show that alternating Fe- and Si-rich bands from the 2.7 billion-year-old Temagami banded iron formation (BIF), Canada, display significantly different ^{142}Nd isotopic compositions. The Fe-rich bands yield a depleted signature (expressed as deviation from the standard in μ notation) with an average μ^{142}Nd of +7.02 ± 0.71, while the Si-rich bands display modern mantle-like signatures (average μ^{142}Nd −2.83 ± 2.32) likely being the results of mixing between different sources. These complementary signatures reflect the dominant, locally derived source of Nd in the seawater at the time of deposition. Our results promote that layering in BIFs is a syn-depositional feature, and that BIFs are unique geochemical archives capable of recording silicate reservoirs that formed during the Hadean but were still extant during the Neoarchean.

Received 30 November 2023 | Accepted 26 April 2024 | Published 30 May 2024

Introduction

The ^{146}Sm-^{142}Nd radiogenic isotope system is the primary tool for tracing early Earth silicate differentiation due to the systems short half-life and decoupling of the parent and daughter elements during silicate differentiation. The parent isotope, ^{146}Sm, was only present during the first ~500 Ma of the solar system, and as such records silicate differentiation during the Hadean. To date, a wide number of (meta)igneous rock samples have been analysed which record μ^{142}Nd anomalies (where $\mu^{142}Nd = \left(\frac{\frac{^{142}Nd}{^{144}Nd_{sample}}}{\frac{^{142}Nd}{^{144}Nd_{standard}}} - 1\right) \times 10^6$), positive if related to the Hadean depleted mantle and negative if derived from a trace element enriched reservoir (Caro *et al.*, 2006, 2017; Bennett *et al.*, 2007; O'Neil *et al.*, 2012, 2016; Rizo *et al.*, 2012, 2013; Debaille *et al.*, 2013; Morino *et al.*, 2017; Schneider *et al.*, 2018; Garcia *et al.*, 2023).

The Superior Craton contains many well preserved and largely unmodified greenstone belts, including the Abitibi and Temagami. The Abitibi Greenstone Belt contains the youngest Archean rock to show a positive ^{142}Nd anomaly, in 2.7 Ga tholeiite lavas (Debaille *et al.*, 2013). The Temagami region has suffered only minor metamorphism (lower greenschist facies; Jolly, 1982) and hosts sedimentary deposits, including banded iron formations (BIF) that give internal Sm-Nd and Lu-Hf isochron ages of 2.7 Ga and for which the ^{143}Nd isotope compositions have been shown to derive from local Abitibi seawater (Viehmann *et al.*, 2014). The banded iron formation at Temagami is a layered marine chemical sediment with alternating bands of Fe-rich magnetite and Si-rich metachert, showing evidence that both high temperature hydrothermal fluids and subaerial terrestrial weathering affected 2.7 Ga Temagami seawater chemistry (Bau and Alexander, 2009; Viehmann *et al.*, 2014; Bau *et al.*, 2022; Mundl-Petermeier *et al.*, 2022). Previous work has shown that the Temagami BIF has unaltered rare earth element (Bau and Alexander, 2009; Supplementary Information), ^{143}Nd and ^{176}Hf isotope compositions (Viehmann *et al.*, 2014). Recently, a multi-proxy approach on the Temagami BIF, using Ge/Si and Th/U ratios as well as Cr isotopes, indicated that the magnetite layers precipitated from ambient seawater with chemistry dominated by hydrothermal fluids, while the (meta)chert layers formed during periods when the ambient seawater chemistry was dominated by continental sources (Bau *et al.*, 2022). As the BIF's trace element composition derives directly from the sources contributing to local seawater, they provide a unique opportunity to investigate the ^{142}Nd composition of these source lithologies at 2.7 Ga. Besides the importance of Nd as the daughter product in both a short lived and long lived chronometer, Nd is also particularly relevant when studying seawater-derived sediments, as its residence time in modern seawater (<700 years; Tachikawa *et al.*, 1999) is significantly shorter than the global mixing time of the oceans (1500 years; Broecker and Peng, 1982). Although the Nd residence time might be somewhat longer in Archean seawater under more reducing atmospheric and hydrospheric conditions and the resulting lack of abundant Fe and Mn (oxyhydr)oxide particles to scavenge REE, Nd and its isotopes are prime geochemical proxies in Archean marine chemical sediments (Viehmann *et al.*, 2015). Hence, they trace the source of components affecting local seawater composition (*e.g.*, Viehmann *et al.*, 2015). This is in marked

1. Laboratoire G-Time, Université Libre de Bruxelles (ULB), Brussels 1050, Belgium
2. School of Geography, Earth and Atmospheric Sciences, University of Melbourne, Parkville 3040, Australia
3. Institute of Geological Sciences, Geochemistry, Freie Universität Berlin, Berlin 12249, Germany
4. Institute of Mineralogy, Leibniz University Hannover, Hannover 30167, Germany
5. CritMET – Critical Metals for Enabling Technologies, School of Science, Constructor University, Bremen 28759, Germany

* Corresponding author (email: awai@unimelb.edu.au)

contrast to the ^{182}W systematics in the Temagami BIF investigated by Mundl-Petermeier *et al.* (2022), where positive μ^{182}W anomalies were observed. While μ^{182}W tracks metal–silicate partitioning and earlier differentiation events than μ^{142}Nd, generally they should show similar trends. The difference in the Temagami BIF can be explained due to tungsten's long residence time in seawater, that exceeds the global mixing time of the oceans. As such, the positive anomalies reported by Mundl-Petermeier *et al.* (2022) represent more global sources, while the μ^{142}Nd discussed here rather represents the local source flux into the seawater.

Methods and Results

Three spatially separate sections of BIF from the Temagami Greenstone Belt were sampled, and homogeneous powders of individual magnetite and metachert layers of each section analysed for high-precision ^{142}Nd. Samples were processed through ion exchange chemistry adapted from the procedures of Debaille *et al.* (2013), prior to 3-lines multi-static analysis by Thermal Ionisation Mass Spectrometer (see Supplementary Information for further details). The raw measurements are corrected for mass fractionation using an exponential law that will account for mass-dependent isotope fractionation. Any possible induced mass-independent fractionation due to nuclear field shift effect during chemical purification is unlikely due to the high Nd yield (>99 %). Sample TM1 shows the largest dissimilarity between the metachert and magnetite layers, with a difference of 10.4 μ units. The two different layers from TM2 are just outside of analytical uncertainty (~4 μ unit) of each other, but the metachert layer is 4.3 μ units lower than the magnetite layer, exceeding the analytical uncertainty. Section TM3 shows the widest variability, with two of the three metachert layers giving an average composition of −3.7 ± 0.19 (2 s.d., error on the average, not analytical error), and one magnetite layer giving +6.6 ± 2.9 (2 s.d.). The two layers TM3-3 and TM3-4 share a similar composition of −0.9 ± 5.1 (2 s.d.) and +1.9 ± 4.1 (2 s.d.) and overlap within uncertainty, despite one being Fe-rich and the other Si-rich (Fig. 1). Due to the similarity of these two adjacent layers, we assume they do not represent a pure end member composition, potentially due to mixing during the resampling process. Therefore, they will not be considered in the following discussion. The Si- and Fe-rich samples of the Temagami BIF define two distinct end member compositions: the metachert bands typically have a lower (negative and close to the present day average) μ^{142}Nd weighted average of −2.5 ± 3.8 (95 % confidence), whereas the magnetite bands are systematically positive with a weighted average of +7.0 ± 1.6 (95 % confidence, Table S-1). However, the ^{142}Nd and ^{143}Nd systematics are decoupled and the samples do not provide any hint on respective source's model age in a two-stage evolution diagram (see Supplementary Information). As observed by Viehmann *et al.* (2014), the ^{143}Nd systematics is below the expected evolution of the depleted MORB mantle (DMM) at 2.7 Ga. With the BIF giving ~+0.2 ± 1.7 ε-unit in the present study (not considering TM1-2), compared to ~+4 for the DMM at 2.7 Ga, this corroborates previous conclusions that both volcanic and more felsic sources affected ancient Temagami seawater. Such decoupling is also to be expected, considering that the ^{142}Nd value of the mantle has stopped growing at 4 Ga, while ^{143}Nd has continued to grow and mix after 4 Ga.

Discussion

We suggest here that the significant difference in ^{142}Nd isotopic compositions between the Fe-rich and Si-rich BIF end members reflects ^{142}Nd input from distinctly different sources that cannot be resolved by the long lived system ^{143}Nd. As such, the short residence time of Nd in seawater allows us to detect this disparate source of the Nd, with the preservation and continued tapping of both, an early depleted reservoir, mostly represented by Fe-rich layers, and a modern-like reservoir, represented by Si layers, at 2.7 Ga. The distinct ^{142}Nd compositions seen in the adjacent BIF bands also strongly support interpretations that the prominent banding in BIFs is a primary depositional feature (for a recent discussion see, *e.g.*, Bau *et al.*, 2022). The ^{182}W results (Mundl-Petermeier *et al.*, 2022) also support the banding as a depositional feature, as the metachert and magnetite layers have distinctly different ^{182}W compositions. Interestingly, the ^{182}W results have excesses in both the metachert and the magnetite layers, with the former showing a stronger excess in ^{182}W. Due to the significantly longer marine residence time of W than Nd (*e.g.*, Sohrin *et al.*, 1987), it is not surprising that the ^{142}Nd and ^{182}W results seem to disagree as they are tracing different mixing scales, with ^{182}W tracing the rather *global* seawater composition and the ^{142}Nd rather tracing *local* input into Temagami seawater.

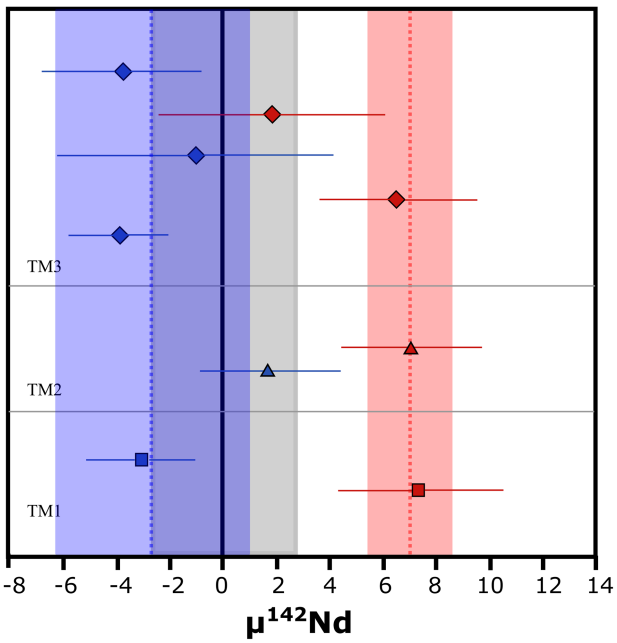

Figure 1 μ^{142}Nd of the Temagami BIF. Blue symbols are Si-rich layers, red symbols are Fe-rich bands. Samples are reproduced in stratigraphic order. All uncertainties are 2 s.d. Light grey band is the 2σ error on the terrestrial standard JNdi, light blue box is the weighted average and error on the chert samples and the light red box is the weighted average and error on the magnetite layer. See text for details.

Remarkably, the ^{142}Nd composition of the depleted end member, with a consistent positive μ^{142}Nd anomaly and a weighted average of +7.0 ± 1.6, perfectly matches the composition of the depleted mantle at 2.7 Ga observed in tholeiites from Theo's Flow, located 200 km north of Temagami (Figs. 1, S-1; Debaille *et al.*, 2013). This provides a highly constrained value for the ^{142}Nd composition of the mantle beneath the Abitibi province at 2.7 Ga. Indeed, this mantle reservoir was not fully homogenised after its formation during the Hadean. It was still an active component during the Neoarchean and contributed positive ^{142}Nd signatures to the seawater from which the Fe-rich bands precipitated, via high temperature hydrothermal fluids that leached submarine volcanics. Interestingly, the 2.7 Ga Boston Creek komatiite flow lies between Theo's Flow and Temagami and has distinctly different μ^{142}Nd of −3.8 ± 2.8 (Puchtel *et al.*, 2018). This flow is unique amongst the Archean komatiites with a deficit in highly siderophile elements

compared to the modern mantle, chondritic $^{187}Os/^{188}Os$ coupled with a positive ^{182}W anomaly. Puchtel *et al.* (2018) concluded that the Boston Creek flow was sourced from a mantle that formed early in Earth's history and was then isolated from the convecting mantle for ≥1.8 billion years. While this would require there to be several heterogeneous mantle domains beneath the Abitibi Greenstone Belt, it supports the conclusion of this study, that the local mantle was not well homogenised and pockets of Hadean-formed mantle remained well into the Neoarchean.

In contrast, the weighted average for the metachert bands is not fully resolvable from the modern homogenised value of 0 ± 3 μ-units, even though it tends towards negative values (Fig. 1). We emphasise, however, that these metachert bands (like most BIF-hosted metacherts) also carry an Fe oxide component which, for example, even dominates the Ga-Al systematics of the metchert bands of the Temagami BIF (Ernst *et al.*, 2023). Hence, the $\mu^{142}Nd$ of −2.5 ± 3.8 for the metachert bands represents a mixture between (i) Nd provided by continental run-off derived from enriched crust and (ii) hydrothermal Nd input from vent fluids that had leached seafloor basalts (*i.e.* depleted mantle), resulting in a 'modern' ^{142}Nd signature.

A negative $\mu^{142}Nd$ value is expected for crust that differentiated from the mantle within the first 500 Myr of the Earth. The extent of this anomaly would depend on both the Sm/Nd ratio of the crust and the age of differentiation, both parameters not being accessible. In addition, erosion results in the mixing of different crustal sources of widely varying age and composition or it could represent the actual composition of the locally derived continental crust, which also contained Eoarchean rocks in the Superior craton (*e.g.*, Böhm *et al.*, 2003). Within seawater, a number of different factors are at play, such as continued input of chemically weathered crustal material mixing with a weakened, but still present, mantle component due to ongoing, but reduced, hydrothermal activity. Regardless, knowing the local mantle was characterised by a $\mu^{142}Nd$ value of +7, obtaining an Archean $\mu^{142}Nd$ value close to 0 requires that locally some crust with negative $\mu^{142}Nd$ was involved in the mixing, and as such was derived from sources that formed while ^{146}Sm was extant, that is, during the Hadean. Intriguingly, the ^{143}Nd systematics of the BIF measured in the present study clearly indicate a mixture between the DMM and an enriched end member (see Supplementary Information) that cannot be identified, while the ^{142}Nd systematics retains a larger spread, with the magnetite bands matching the composition of the DMM at 2.7 Ga. However, modelling of this mixing cannot be performed in absence of Nd concentrations of the respective end members, especially in seawater. Following the approach (Fig. 2) of O'Neil and Carlson (2017), and considering that ^{142}Nd can directly identify the enriched end member, its minimum differentiation age from a mafic precursor should be late (~4.1 Ga). This suggests a time span of at least 1.4 Ga for the longevity of the Hadean crust, implying a low recycling rate.

Implications of Archean mantle geodynamics

The Neoarchean is considered by some to be a transitional period from a stagnant lid to a plate tectonic-like global regime (Debaille *et al.*, 2013; Cawood *et al.*, 2018), with evidence of this seen in parts of the Superior Craton where there are cyclic subduction episodes and periods of stagnant lid quiescence (Wyman, 2018). It is also the time of amalgamation of the Superior Craton, which happened during the formation of the Temagami BIF (Wyman, 2018). Nevertheless, there has been much debate about how the Abitibi Greenstone Belt formed,

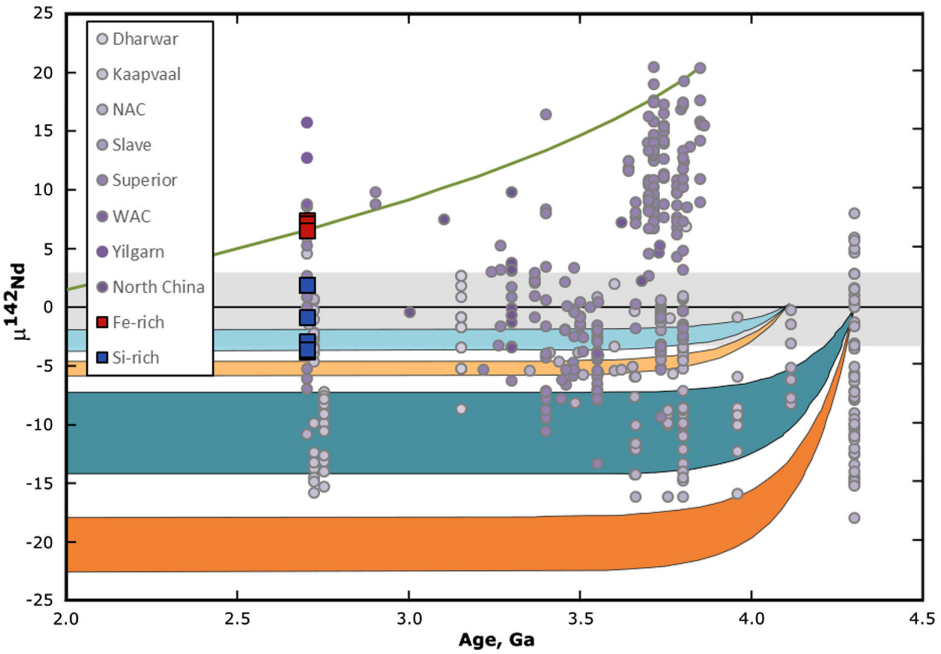

Figure 2 Model showing the evolution of $\mu^{142}Nd$ through time, based on extraction of a Tonalite-Trondhjemite-Granodiorite (TTG) from a mafic (blue) or felsic (orange shaded area) source at 4.3 and 4.1 Ga (from O'Neil and Carlson, 2017). Model was calculated using the approach of Morino *et al.* (2017), using a modern-like terrestrial ^{142}Nd composition as the bulk Earth, with a $\mu^{142}Nd$ of 0. Squares are data from this work, circles are the available ^{142}Nd literature data (Caro *et al.*, 2006, 2017, Bennett *et al.*, 2007; O'Neil *et al.*, 2008, 2012, 2016; Rizo *et al.*, 2012, 2013; Debaille *et al.*, 2013; Puchtel *et al.*, 2013, 2016; Roth *et al.*, 2013, 2014; Li *et al.*, 2017; Maya *et al.*, 2017; Morino *et al.*, 2017; O'Neil and Carlson, 2017; Schneider *et al.*, 2018; Wainwright *et al.*, 2019). The green line is the model from Debaille *et al.* (2013) showing trend of mixing in the mantle required to progress from the most positive values at 3.8 Ga to the +7 found in Abitibi at 2.7 Ga.

with two competing theories involving cyclic subduction or a mantle plume (van Hunen and Moyen, 2012; Wyman, 2018). While the data obtained in this study cannot exclude either of these hypotheses, it suggests that any subduction that could have occurred, should have only been short lived as it was unable to destroy all early crust (*e.g.*, by erosion of uplifted continental margins) and to homogenise the depleted mantle reservoir—at least until 2.7 Ga. As such, the preservation of a depleted mantle reservoir and an enriched continental crust at 2.7 Ga in the Abitibi is of great significance. It reveals that, in spite of intense mantle convection (Debaille *et al.*, 2013, and references therein) and magmatic activity, any global homogenisation process in the Archean was slow, and that BIF and potentially other chemical sediments that are derived from seawater are important archives able to trace early formed Hadean silicate reservoirs even during the Archean.

Acknowledgements

S. Cauchies is thanked for lab support. ANW and VD thank the ERC StG 336718 "ISoSyc" for financial support. VD also thanks the FRS-FNRS for support. SV acknowledges FWF project P34238. The authors also thank two anonymous reviewers for helping to improve this manuscript.

Editor: Helen Williams

Additional Information

Supplementary Information accompanies this letter at https://www.geochemicalperspectivesletters.org/article2421.

Cite this letter as: Wainwright, A.N., Debaille, V., Hoffmann, J.E., Viehmann, S., Bau, M. (2024) Neoarchean marine chemical sediments as archives of Hadean silicate differentiation. *Geochem. Persp. Let.* 30, 46–50. https://doi.org/10.7185/geochemlet.2421

References

Bau, M., Alexander, B.W. (2009) Distribution of high field strength elements (Y, Zr, REE, Hf, Ta, Th, U) in adjacent magnetite and chert bands and in reference standards FeR-3 and FeR-4 from the Temagami iron-formation, Canada, and the redox level of the Neoarchean ocean. *Precambrian Research* 174, 337–346. https://doi.org/10.1016/j.precamres.2009.08.007

Bau, M., Frei, R., Garbe-Schönberg, D., Viehmann, S. (2022) High-resolution Ge-Si-Fe, Cr isotope and Th-U data for the Neoarchean Temagami BIF, Canada, suggest primary origin of BIF bands and oxidative terrestrial weathering 2.7 Ga ago. *Earth and Planetary Science Letters* 589, 117579. https://doi.org/10.1016/j.epsl.2022.117579

Bennett, V.C., Brandon, A.D., Nutman, A.P. (2007) Coupled ^{142}Nd-^{143}Nd Isotopic Evidence for Hadean Mantle Dynamics. *Science* 318, 1907–1910. https://doi.org/10.1126/science.1145928

Böhm, C.O., Heaman, L.M., Stern, R.A., Corkery, M.T., Creaser, R.A. (2003) Nature of assean lake ancient crust, Manitoba: a combined SHRIMP–ID-TIMS U–Pb geochronology and Sm–Nd isotope study. *Precambrian Research* 126, 55–94. https://doi.org/10.1016/S0301-9268(03)00127-X

Broecker, W.S., Peng, T.-H. (1982) *Tracers in the Sea* (*vol. 690*). Lamont-Doherty Geological Observatory, Columbia University, Palisades, New York.

Caro, G., Bourdon, B., Birck, J.-L., Moorbath, S. (2006) High-precision ^{142}Nd/^{144}Nd measurements in terrestrial rocks: Constraints on the early differentiation of the Earth's mantle. *Geochimica et Cosmochimica Acta* 70, 164–191. https://doi.org/10.1016/j.gca.2005.08.015

Caro, G., Morino, P., Mojzsis, S.J., Cates, N.L., Bleeker, W. (2017) Sluggish Hadean geodynamics: Evidence from coupled ^{146,147}Sm–^{142,143}Nd systematics in Eoarchean supracrustal rocks of the Inukjuak domain (Québec). *Earth and Planetary Science Letters* 457, 23–37. https://doi.org/10.1016/j.epsl.2016.09.051

Cawood, P.A., Hawkesworth, C.J., Pisarevsky, S.A., Dhuime, B., Capitanio, F.A., Nebel, O. (2018) Geological archive of the onset of plate tectonics. *Philosophical Transactions of the Royal Society A: Mathematical, Physical and Engineering Sciences* 376, 20170405. https://doi.org/10.1098/rsta.2017.0405

Debaille, V., O'Neill, C., Brandon, A.D., Haenecour, P., Yin, Q.-Z., Mattielli, N., Treiman, A.H. (2013) Stagnant-lid tectonics in early Earth revealed by ^{142}Nd variations in late Archean rocks. *Earth and Planetary Science Letters* 373, 83–92. https://doi.org/10.1016/j.epsl.2013.04.016

Ernst, D.M., Garbe-Schönberg, D., Kraemer, D., Bau, M. (2023) A first look at the gallium-aluminium systematics of Early Earth's seawater: Evidence from Neoarchean banded iron formation. *Geochimica et Cosmochimica Acta* 355, 48–61. https://doi.org/10.1016/j.gca.2023.06.019

Garcia, V.B., O'Neil, J., Dantas, E.L. (2023) Rare evidence for the existence of a Hadean enriched mantle reservoir. *Geochemical Perspectives Letters* 28, 1–6 https://doi.org/10.7185/geochemlet.2336

Jolly, W. (1982) Progressive Metamorphism of Komatiites and rekated Archean lavas of the Abibiti area, Canada. In: Arndt, N.T., Nisbet, E.G. (Eds.) *Komatiites*. George Allen and Unwin, London, 245–266.

Li, C.-F., Wang, X.-C., Wilde, S.A., Li, X.-H., Wang, Y.-F., Li, Z. (2017) Differentiation of the early silicate Earth as recorded by ^{142}Nd-^{143}Nd in 3.8–3.0Ga rocks from the Anshan Complex, North China Craton. *Precambrian Research* 301, 86–101. https://doi.org/10.1016/j.precamres.2017.09.001

Maya, J.M., Bhutani, R., Balakrishnan, S., Rajee Sandhya, S. (2017) Petrogenesis of 3.15 Ga old Banasandra komatiites from the Dharwar craton, India: Implications for early mantle heterogeneity. *Geoscience Frontiers* 8, 467–481. https://doi.org/10.1016/j.gsf.2016.03.007

Morino, P., Caro, G., Reisberg, L., Schumacher, A. (2017) Chemical stratification in the post-magma ocean Earth inferred from coupled ^{146,147}Sm–^{142,143}Nd systematics in ultramafic rocks of the Saglek block (3.25–3.9 Ga; northern Labrador, Canada). *Earth and Planetary Science Letters* 463, 136–150. https://doi.org/10.1016/j.epsl.2017.01.044

Mundl-Petermeier, A., Viehmann, S., Tusch, J., Bau, M., Kurzweil, F., Münker, C. (2022) Earth's geodynamic evolution constrained by ^{182}W in Archean seawater. *Nature Communications* 13, 2701. https://doi.org/10.1038/s41467-022-30423-3

O'Neil, J., Carlson, R.W., Francis, D., Stevenson, R.K. (2008) Neodymium-142 Evidence for Hadean Mafic Crust. *Science* 321, 1828–1831. https://doi.org/10.1126/science.1161925

O'Neil, J., Carlson, R.W., Paquette, J.-L., Francis, D. (2012) Formation age and metamorphic history of the Nuvvuagittuq Greenstone Belt. *Precambrian Research* 220–221, 23–44. https://doi.org/10.1016/j.precamres.2012.07.009

O'Neil, J., Rizo, H., Boyet, M., Carlson, R.W., Rosing, M.T. (2016) Geochemistry and Nd isotopic characteristics of Earth's Hadean mantle and primitive crust. *Earth and Planetary Science Letters* 442, 194–205. https://doi.org/10.1016/j.epsl.2016.02.055

O'Neil, J., Carlson, R.W. (2017) Building Archean cratons from Hadean mafic crust. *Science* 355, 1199–1202. https://doi.org/10.1126/science.aah3823

Puchtel, I.S., Blichert-Toft, J., Touboul, M., Walker, R.J., Byerly, G.R., Nisbet, E.G., Anhaeusser, C.R. (2013) Insights into early Earth from Barberton komatiites: Evidence from lithophile isotope and trace element systematics. *Geochimica et Cosmochimica Acta* 108, 63–90. https://doi.org/10.1016/j.gca.2013.01.016

Puchtel, I.S., Blichert-Toft, J., Touboul, M., Horan, M.F., Walker, R.J. (2016) The coupled ^{182}W-^{142}Nd record of early terrestrial mantle differentiation. *Geochemistry, Geophysics, Geosystems* 17, 2168–2193. https://doi.org/10.1002/2016GC006324

Puchtel, I.S., Blichert-Toft, J., Touboul, M., Walker, R.J. (2018) ^{182}W and HSE constraints from 2.7 Ga komatiites on the heterogeneous nature of the Archean mantle. *Geochimica et Cosmochimica Acta* 228, 1–26. https://doi.org/10.1016/j.gca.2018.02.030

Rizo, H., Boyet, M., Blichert-Toft, J., O'Neil, J., Rosing, M.T., Paquette, J.-L. (2012) The elusive Hadean enriched reservoir revealed by ^{142}Nd deficits in

Isua Archaean rocks. *Nature* 491, 96–100. https://doi.org/10.1038/nature11565

Rizo, H., Boyet, M., Blichert-Toft, J., Rosing, M.T. (2013) Early mantle dynamics inferred from 142Nd variations in Archean rocks from southwest Greenland. *Earth and Planetary Science Letters* 377–378, 324–335. https://doi.org/10.1016/j.epsl.2013.07.012

Roth, A.S.G., Bourdon, B., Mojzsis, S.J., Touboul, M., Sprung, P., Guitreau, M., Blichert-Toft, J. (2013) Inherited ^{142}Nd anomalies in Eoarchean protoliths. *Earth and Planetary Science Letters* 361, 50–57. https://doi.org/10.1016/j.epsl.2012.11.023

Roth, A.S.G., Bourdon, B., Mojzsis, S.J., Rudge, J.F., Guitreau, M., Blichert-Toft, J. (2014) Combined ^{147,146}Sm-^{143,142}Nd constraints on the longevity and residence time of early terrestrial crust. *Geochemistry, Geophysics, Geosystems* 15, 2329–2345. https://doi.org/10.1002/2014GC005313

Schneider, K.P., Hoffmann, J.E., Boyet, M., Münker, C., Kröner, A. (2018) Coexistence of enriched and modern-like ^{142}Nd signatures in Archean igneous rocks of the eastern Kaapvaal Craton, southern Africa. *Earth and Planetary Science Letters* 487, 54–66. https://doi.org/10.1016/j.epsl.2018.01.022

Sohrin, Y., Isshiki, K., Kuwamoto, T., Nakayama, E. (1987) Tungsten in north pacific waters. *Marine Chemistry* 22, 95–103. https://doi.org/10.1016/0304-4203(87)90051-X

Tachikawa, K., Jeandel, C., Roy-Barman, M. (1999) A new approach to the Nd residence time in the ocean: the role of atmospheric inputs. *Earth and Planetary Science Letters* 170, 433–446. https://doi.org/10.1016/S0012-821X(99)00127-2

van Hunen, J., Moyen, J.-F. (2012) Archean Subduction: Fact or Fiction? *Annual Review of Earth and Planetary Sciences* 40, 195–219. https://doi.org/10.1146/annurev-earth-042711-105255

Viehmann, S., Hoffmann, J.E., Münker, C., Bau, M. (2014) Decoupled Hf-Nd isotopes in Neoarchean seawater reveal weathering of emerged continents. *Geology* 42, 115–118. https://doi.org/10.1130/G35014.1

Viehmann, S., Bau, M., Hoffmann, J.E., Münker, C. (2015) Geochemistry of the Krivoy Rog Banded Iron Formation, Ukraine, and the impact of peak episodes of increased global magmatic activity on the trace element composition of Precambrian seawater. *Precambrian Research* 270, 165–180. https://doi.org/10.1016/j.precamres.2015.09.015

Wainwright, A.N., El Atrassi, F., Debaille, V., Mattielli, N. (2019) Geochemistry and petrogenesis of Archean mafic rocks from the Amsaga area, West African craton, Mauritania. *Precambrian Research* 324, 208–219. https://doi.org/10.1016/j.precamres.2019.02.005

Wyman, D. (2018) Do cratons preserve evidence of stagnant lid tectonics? *Geoscience Frontiers* 9, 3–17. https://doi.org/10.1016/j.gsf.2017.02.001

Geochemical Perspectives Letters

Neoarchean marine chemical sediments as archives of Hadean silicate differentiation

A.N. Wainwright, V. Debaille, J.E. Hoffmann, S. Viehmann, M. Bau

Supplementary Information

The Supplementary Information includes:

- Regional geology and sample description
- Methods
- Trace Elements
- $^{143}Nd/^{144}Nd$ modelling
- Tables S-1 to S-3
- Figures S-1 to S-5
- Supplementary Information References

Regional geology and sample description

The Temagami BIF is part of the Temagami Greenstone Belt that is located in the Neoarchean Abitibi Greenstone succession, Ontario, Canada. The up to 200 m thick Algoma-type BIF is associated with (meta)sedimentary and (meta)volcanic units (Fig. S-1). The here studied BIF samples originate from a road cut on Highway 11 north of the village of Temagami (47°04‘24’’ N; 79°47’31’’ W). The BIF consist of alternating chert and magnetite mesobands (Fig. S-2) and experienced only lower greenschist facies metamorphism (Fyon and Cole, 1989). Both magnetite and chert bands show no geochemical evidence for detrital aluminosilicate contamination (Bau and Alexander, 2009; Viehmann *et al.,* 2014; Bau *et al.,* 2022; Mundl-Petermeier *et al.,* 2022). The depositional age of the BIF is bracketed by U-Pb zircon ages of 2736 ± 3 Ma from underlying metavolcanics and 2687 ± 2 Ma of a crosscutting rhyolitic dyke (Bowins and Heaman, 1991). Individual chert and magnetite bands of the BIF were recently directly dated via the radiogenic Sm-Nd and Lu-Hf isotopes and yield 2605 ± 140 Ma and 2760 ± 120 Ma, respectively, overlapping with the proposed depositional age and suggesting negligible impact of post-depositional overprints (Viehmann *et al.,* 2014).

Methods

In sections TM1 and TM2 two adjacent layers were analysed, while in section TM3 five adjacent layers (3 chert and 2 magnetite) were analysed. Due to the large amount of sample powder required for these analyses, all samples were re-sampled from previous studies (Bau and Alexander, 2009; Viehmann *et al.,* 2014), but are similar to those used in

Mundl-Petermeier *et al*. (2022). Individual chert and magnetite were separated by a diamond saw and then homogenised in an agate mill. This technique could have resulted in less pristine separation relative to micro-drill samples, for example for samples TM 3-3 and TM3-4 that are suspected to have been mixed, possibly due to the faulting in the sample (see Fig. S-3).

Approximately 1 g of each sample were weighed and digested using a mixture of concentrated HNO_3 and HF followed by HCl in closed Savillex beakers. After digestion a 5% aliquot was taken for isotope dilution analysis of Nd and Sm. The remaining solution was processed for unspiked Nd compositions; the separation procedure used was adapted from Debaille *et al.* (2013). In brief, five separate columns are used to purify Nd from Ce and Sm. Firstly, Fe is removed with anion resin, then the Nd was purified from the matrix first with ~2 ml of AG50W-X8 cation resin (200-400 mesh). The matrix was eluted in 2N HCl and the REE cut was collected in 6N HCl. This was subsequently purified by HDEHP (di-2ethylhexyl-orthophosphoric acid)-coated Teflon powder where a Nd cut was obtained containing traces of Ce. For ensuring efficient removal of Ce from the Nd cut due to the isobaric interference on mass 142, a second HDEP column was used following the procedure of Li *et al.* (2015). In brief, Ce is oxidised as Ce^{4+} using NaBrO3 in HNO3 and as such sticks on the HDEHP resin, while Nd in 3+ state is eluted. The final column used 0.5 ml of AG50X8 resin, to remove the Na added during the Ce clean-up column, recovering Nd in 6N HCl. The total recovery of Nd was better than 99%, hence avoiding any potential nuclear field shift effect (Saji *et al.,* 2016). Total procedural blanks are 72 ppt of Nd and 15 ppt of Sm.

The isotope dilution aliquots are spiked with a ^{150}Sm-^{148}Nd mixed spike. Neodymium and Sm were purified from the matrix using a two-column ion-exchange technique as detailed in Debaille *et al.* (2013). First, a column composed of ~2 ml of AG50W-X8 cation resin (200-400 mesh) separates the REE the matrix. The REE are then processed over a HDEHP (di-2ethylhexyl-orthophosphoric acid)-coated Teflon powder column for the purification of Nd and Sm from the remaining matrix.

High precision ^{142}Nd was measured with a Thermo Scientific Triton Plus TIMS at the Laboratoire G-Time (ULB). Samples were measured as Nd metal on Re double filaments. Total measurements consisted of 18-54 blocks of 20 cycles, with an intensity on ^{142}Nd greater than 3V and rotating the amplifiers. Each measurement cycle consisted of a multi-static sequence across 3-lines (see Table S-2) following the method of Caro *et al.* (2006), Debaille *et al.* (2007) and Debaille *et al.* (2013) to ensure that differences in Faraday cup efficiency are cancelled and that all isobaric interferences could be monitored. Ratios are calculated for each line, which are subsequently corrected for mass fractionation via the exponential law, with all ratios corrected to ^{146}Nd/^{144}Nd of 0.7219. Cerium and Sm corrections are then applied, and final corrected ratios calculated for each individual line. The reported data is the average for each ratio across all three lines for each individual measurement (i.e. one round of all three lines being measured). This method also allows for the high precision measurement of ^{143}Nd. Isobaric interferences from Sm and Ce were minimal, with the largest Ce correction applied of 3 ppm. International reference material JNdi was run alongside the samples, with a reproducibility of μ^{142}Nd= 0.0 ± 2.0 during this analytical campaign (2σ, n=5).

Trace Elements

While the samples analysed in this work are the same as those from previous workers (Bau and Alexander, 2009; Viehmann *et al.,* 2014), the actual drilled samples are a separate aliquot, having been milled from the whole rock at separate times. As such, we performed trace element analyses when enough powder was left to ensure that there were no significant differences between the powder aliquots. Figure S-4 shows the chondrite normalised rare earth element data from this study (solid lines) and from Viehmann *et al.,* 2014 (dashed lines) for four samples. The measurements

are in good agreement except TM 3-5 showing the largest offset between the two studies, likely due to the resampling process. The remaining three samples are within the limits of inter-lab comparisons and uncertainty. Refer to Table S-3 for full trace element results.

$^{143}Nd/^{144}Nd$ Modelling

The ^{142}Nd and ^{143}Nd systematics are decoupled as they do not plot in the field defined by a two-stage model evolution (not shown). As such, the samples do not provide any hint on the timing of source model ages. In addition, Viehmann *et al.* (2014) already observed that the ^{143}Nd systematics is below the expected evolution of the depleted MORB mantle (DMM), ~+0.2 ± 1.7 ε-unit for the BIF in the present study (not considering TM 1-2 outlying at +10), compared to ~+4 for the DMM at 2.7 Ga, providing evidence that both volcanic and more felsic sources affected ancient Temagami seawater. Previous studies have shown decoupling of the $^{143\text{-}142}Nd$ systems, most notably in the Acasta Gneisses (Roth *et al.,* 2014), Nuvvuagittuq supracrustal belt (O'Neil *et al.,* 2008, 2012), Ameralik dykes (Rizo *et al.,* 2012) and the Schapenburg komatiite (Puchtel *et al.,* 2016). This decoupling can be attributed to a variety of factors, such as Sm/Nd fractionation after extinction of ^{146}Sm, or disturbance of the ^{147}Sm-^{143}Nd system. Therefore, it is not unusual for the $^{143\text{-}142}Nd$ systems to be decoupled in the Temagami BIF, which is also exacerbated by the likely multiple source components that are mixed into the seawater to provide the Nd compositions seen. While it is possible to have the ^{147}Sm-^{143}Nd system to be disturbed by later events, one should not assume that the ^{142}Nd systematic is always pristine. Indeed, we show here that the ^{142}Nd signature in the chert is likely a mixture between different continental sources with mantle hydrothermal-venting input. This is possibly the result of a changing activity and quiescence in the hydrothermal activity in the region surrounding the BIF deposition.

Supplementary Tables

Table S-1 **(over page)** Sm-Nd results for the Temagami BIF, and JNdi standards.

Sample	Lithology	Sm, ppm	Nd, ppm	ppm 142 Ce	142Nd/144Nd	2SD	143Nd/144Nd	2SD	145Nd/144Nd	2SD	146Nd/144Nd raw	148Nd/144Nd	2SD	150Nd/144Nd	2SD	147Sm/144Nd	u142Nd	2SD	143Nd/144Ndi	eNd
JNdi	standard	-	-	0.5	1.1418350	3E-06	0.512099	1E-06	0.348404	7E-07	0.722340	0.241579	1E-06	0.236449	2E-06	-	-	-	-	-
JNdi	standard	-	-	1.3	1.1418327	4E-06	0.512100	1E-06	0.348404	8E-07	0.722612	0.241580	1E-06	0.236449	2E-06	-	-	-	-	-
JNdi	standard	-	-	0.9	1.1418322	3E-06	0.512099	1E-06	0.348403	7E-07	0.721751	0.241578	9E-07	0.236448	2E-06	-	-	-	-	-
JNdi	standard	-	-	0.4	1.1418334	3E-06	0.512098	1E-06	0.348404	7E-07	0.721800	0.241580	1E-06	0.236448	2E-06	-	-	-	-	-
JNdi	standard	-	-	1.1	1.1418344	3E-06	0.512100	1E-06	0.348403	6E-07	0.722000	0.241579	1E-06	0.236447	2E-06	-	-	-	-	-
JNdi average				**0.8**	**1.1418335**	**2E-06**	**0.512099**	**1E-06**	**0.348404**	**9E-07**	**0.722101**	**0.241579**	**1E-06**	**0.236448**	**1E-06**					
TM 1-1	Fe-rich	0.79	4.33	0.9	1.1418417	3E-06	0.511053	1E-06	0.348404	9E-07	0.723021	0.241579	1E-06	0.236449	2E-06	0.1077	7.4	3.0	0.509134	0.0
TM 1-2	Chert	0.13	0.76	0.6	1.1418305	2E-06	0.511432	8E-07	0.348403	5E-07	0.722084	0.241577	7E-07	0.236444	1E-06	0.1003	-3.0	2.0	0.509646	10.0
TM 2-2	Chert	0.28	1.1	1.0	1.1418360	3E-06	0.511794	1E-06	0.348403	7E-07	0.722065	0.241578	1E-06	0.236444	2E-06	0.1481	1.9	2.6	0.509156	0.4
TM 2-3	Fe-rich	1.04	5.34	1.0	1.1418414	3E-06	0.511143	1E-06	0.348403	7E-07	0.722529	0.241578	1E-06	0.236449	2E-06	0.1151	7.1	2.6	0.509093	-0.8
TM 3-1	Chert	0.52	2.44	2.7	1.1418296	2E-06	0.511449	8E-07	0.348404	5E-07	0.720923	0.241576	8E-07	0.236440	1E-06	0.1264	-3.8	1.8	0.509198	1.2
TM 3-2	Fe-rich	1.19	6.16	2.2	1.1418408	3E-06	0.511181	1E-06	0.348403	8E-07	0.723009	0.241579	1E-06	0.236448	2E-06	0.1134	6.6	2.9	0.509160	0.5
TM 3-3*	Chert	0.13	0.6	1.9	1.1418329	6E-06	0.511473	2E-06	0.348404	1E-06	0.723505	0.241587	2E-06	0.236447	4E-06	0.1295	-0.9	5.1	0.509167	0.6
TM 3-4*	Fe-rich	0.82	4.07	3.2	1.1418354	5E-06	0.511198	2E-06	0.348403	1E-06	0.721464	0.241577	2E-06	0.236442	3E-06	0.1190	1.9	4.2	0.509079	-1.1
TM 3-5	Chert	0.11	0.56	0.5	1.1418297	3E-06	0.511287	1E-06	0.348403	7E-07	0.722124	0.241580	1E-06	0.236442	2E-06	0.1178	-3.7	2.9	0.509188	1.0
Chert weighted average																	**-2.5**	**3.8**		
Fe-rich weighted average																	**7.0**	**1.6**		

*not included in average calculations

Table S-2 Cup configuration of each line for ^{142}Nd TIMS measurement

Cup	L4	L3	L2	L1	Center	H1	H2	H3	H4
Line 1	^{140}Ce	^{142}Nd	^{143}Nd	^{144}Nd	^{145}Nd	^{146}Nd	^{147}Sm	^{148}Nd	^{150}Nd
Line 2		^{141}Pr	^{142}Nd	^{143}Nd	^{144}Nd	^{145}Nd	^{146}Nd	^{147}Sm	
Line 3		^{140}Ce	^{141}Pr	^{142}Nd	^{143}Nd	^{144}Nd	^{145}Nd	^{146}Nd	^{148}Nd

Table S-3 Trace element results for 4 of the samples analysed for ^{142}Nd along with analysis of reference material BHVO2 (Hawaiian Volcano Observatory Basalt).
Table S-3 is available for download (.xlsx) from the online version of this article at http://doi.org/10.7185/geochemlet.2421.

Supplementary Figures

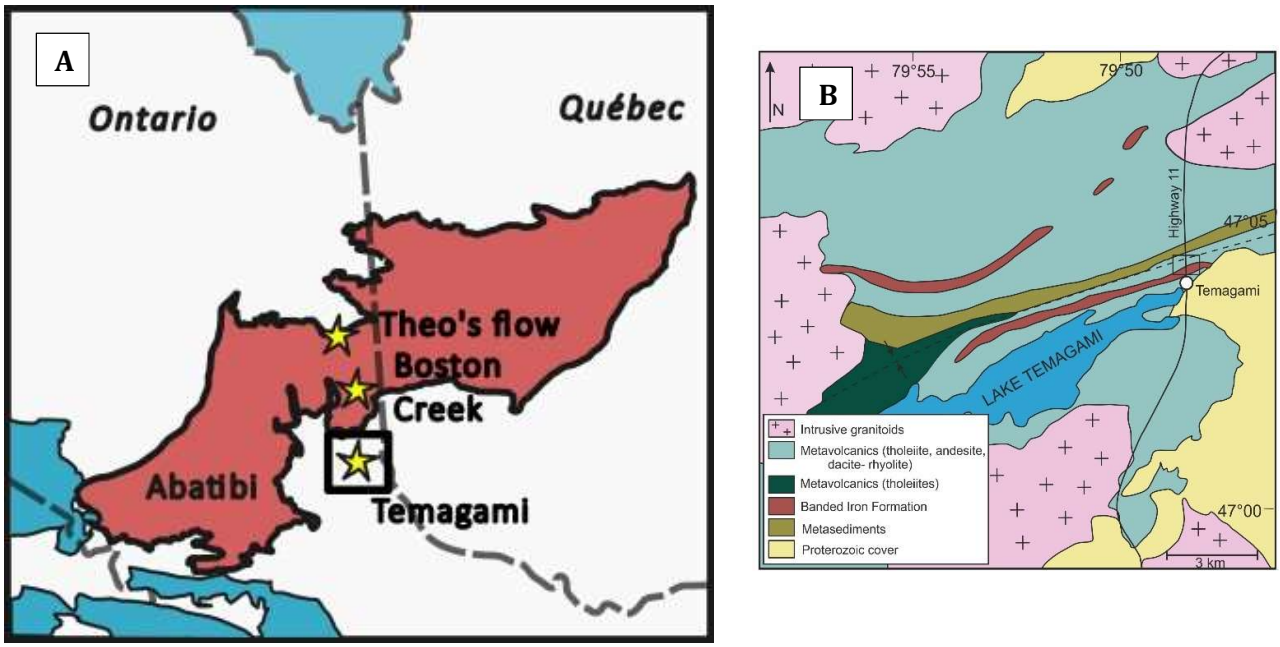

Figure S-1 **A)** Regional map of the Abibiti Greenstone belt in Canada, stars show locations of Theo's Flow (Debaille *et al.,* 2013), Boston Creek Komatiite (Puchtel *et al.,* 2018) and the Temagami. Square around Temagmi is region shown in panel b. **B)** Simplified geological map of the Temagami Greenstone Belt (modified from Bowins and Crocket, 1994; Bau *et al.,* 2022)

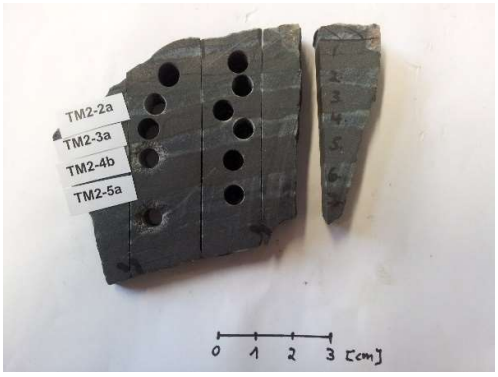

Figure S-2 Representative Temagami BIF sample with alternating chert and magnetite layers

Figure S-3 Photo of TM3 hand specimen, prior to sawing and milling for this study. As can be seen in the image, the hand samples shows small fractures and faults, which allows for the mixing of sample layers. During sampling it is possible that one of these areas was inadvertently sampled, leading to the similar ^{142}Nd compositions of TM3-3 and TM3-4.

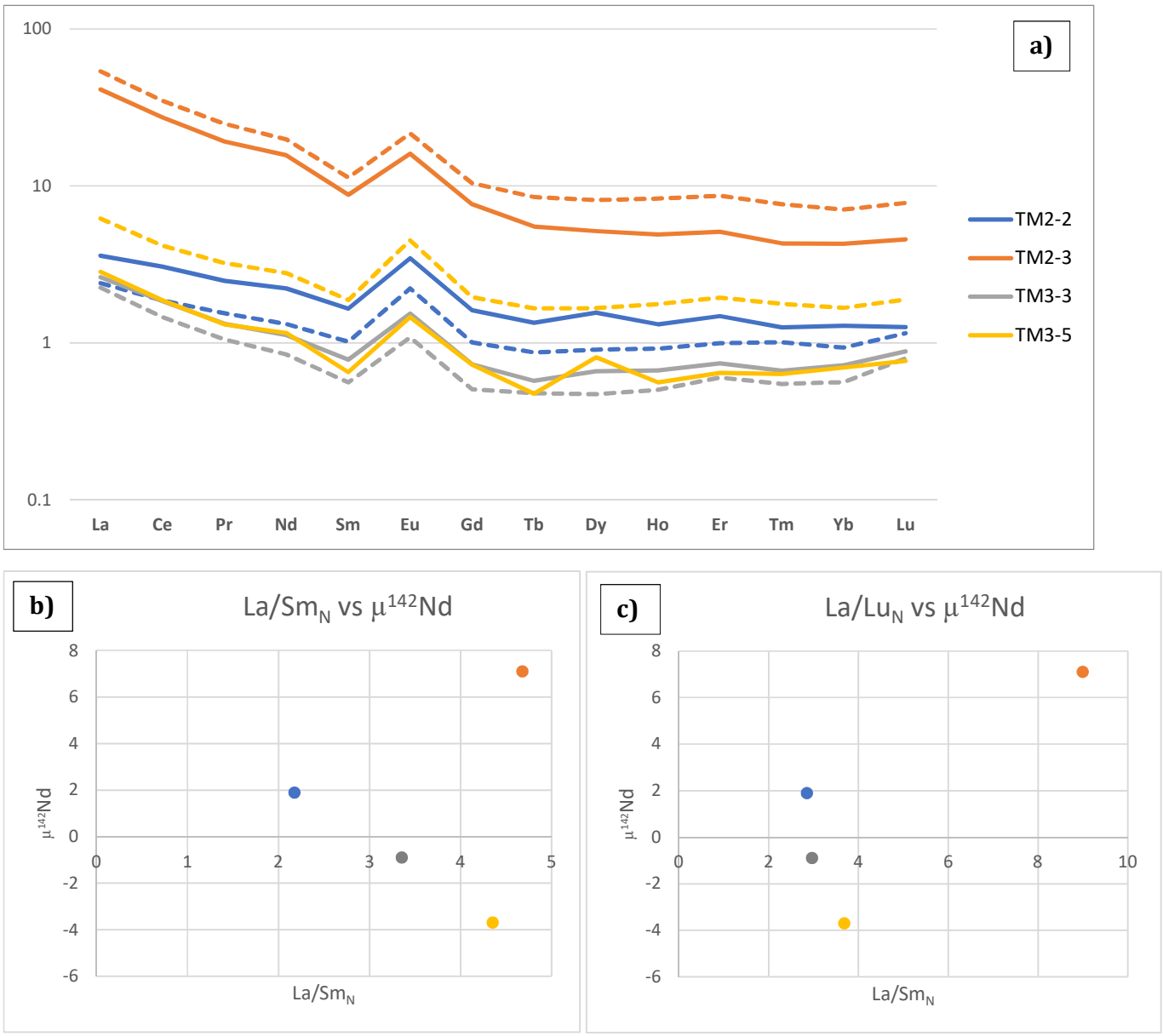

Figure S-4 **a)** Chondrite normalised rare earth element plots for four samples, comparing this study's results to previous work (Viehmann *et al.,* 2014), due to this study using re-sampled powders. The majority of samples are within analytical uncertainty and inter-lab comparisons expected for trace element results (± 10%). **b) and c)** La/Sm_N vs $\mu^{142}Nd$ and La/Lu_N vs $\mu^{142}Nd$ plots, for the same for samples as in a. Showing no correlation between trace elements and ^{142}Nd compositions.

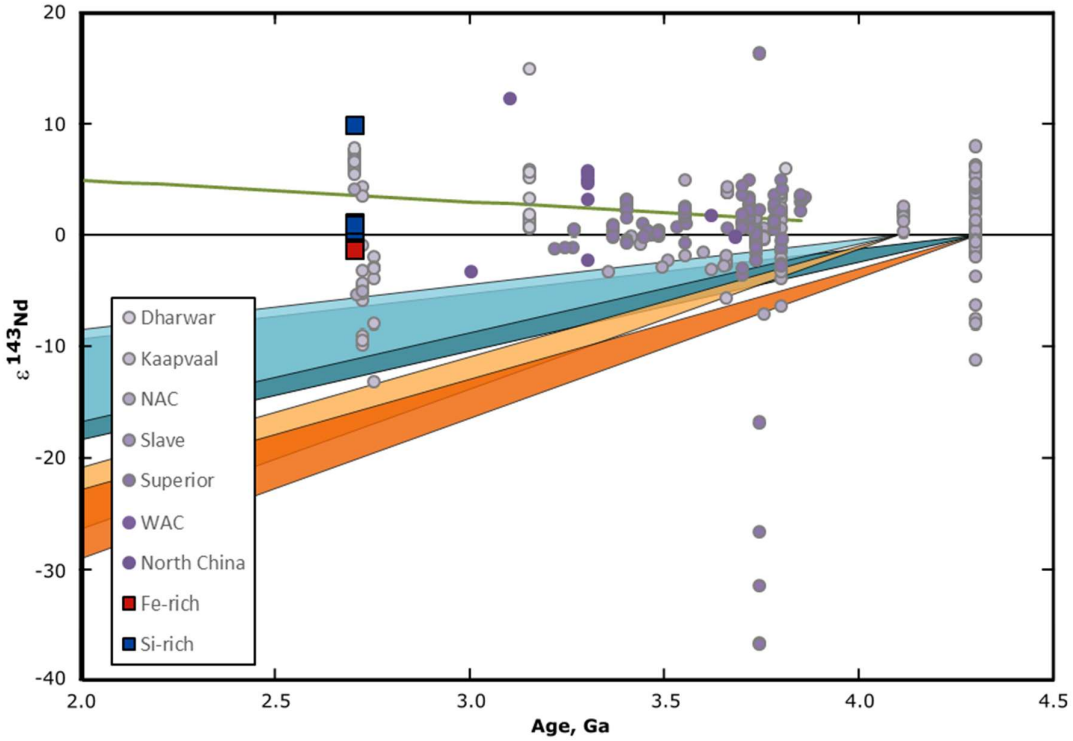

Figure S-5 Model showing the evolution of ε^{143}Nd through time, based on extraction of a TTG from a mafic (blue shaded areas) or felsic (orange shaded areas) source at 4.3 and 4.1 Ga. Model was calculated using a chondritic ^{147}Sm-^{143}Nd composition (from Bouvier *et al.,* 2008). Squares are data from this work, circles are the available ^{143}Nd literature data for samples that have also been analysed for ^{142}Nd. Dark green line is model from Debaille *et al.* (2013) showing trend of mixing in the mantle required to progress from the most positive ^{142}Nd values at 3.8 Ga to the +7 found in Abitibi at 2.7 Ga. (Caro *et al.,* 2003, 2017; Bennett *et al.,* 2007; O'Neil *et al.,* 2008, 2012, 2016; Rizo *et al.,* 2011, 2012; Debaille *et al.,* 2013; Puchtel *et al.,* 2013, 2016; Li *et al.,* 2017; Maya *et al.,* 2017; Morino *et al.,* 2017; Schneider *et al.,* 2018; O'Neil and Carlson, 2017; Wainwright *et al.,* 2019). Note that for the modelling (Fig. 2 and Fig. S-3.), we have used the approach of Morino *et al.* (2017) with bulk Earth (i.e. starting off point of the differentiation model) having a chondritic ^{143}Nd value but a terrestrial modern-like ^{142}Nd value.

Supplementary Information References

Bau, M., Alexander, B.W. (2009) Distribution of high field strength elements (Y, Zr, REE, Hf, Ta, Th, U) in adjacent magnetite and chert bands and in reference standards FeR-3 and FeR-4 from the Temagami iron-formation, Canada, and the redox level of the Neoarchean ocean. *Precambrian Research* 174, 337–346. https://doi.org/10.1016/j.precamres.2009.08.007

Bau, M., Frei, R., Garbe-Schönberg, D., Viehmann, S. (2022) High-resolution Ge-Si-Fe, Cr isotope and Th-U data for the Neoarchean Temagami BIF, Canada, suggest primary origin of BIF bands and oxidative terrestrial weathering 2.7 Ga ago. *Earth and Planetary Science Letters* 589, 117579. https://doi.org/10.1016/j.epsl.2022.117579

Bennett, V.C., Brandon, A.D., Nutman, A.P. (2007) Couple ^{142}Nd-^{143}Nd Isotopic Evidence for Hadean Mantle Dynamics. *Science* 318, 1907-1910. https://doi.org/10.1126/science.1145928

Bouvier, A., Vervoort, J.D., Patchett, P.J. (2008) The Lu-Hf and Sm-Nd isotopic composition of CHUR: Constraints from unequilibrated chondrites and implications for the bulk composition of terrestrial planets. *Earth and Planetary Science Letters* 273, 48-57. https://doi.org/10.1016/j.epsl.2008.06.010

Bowins, R.J., Heaman, L.M. (1991) Age and timing of igneous activity in the Temagami greenstone belt, Ontario: A preliminary report. *Canadian Journal of Earth Sciences* 28, 1873–1876. https://doi.org/10.1139/e91-167

Bowins, R.J., Crocket, J.H. (1994) Sulfur and carbon isotopes in Archean banded iron formations: Implications for sulfur sources. *Chemical Geology* 111, 307-323. https://doi.org/10.1016/0009-2541(94)90097-3

Caro, G., Bourdon, B., Birck, J-L., Moorbath, S. (2003) ^{146}Sm-^{142}Nd evidence from Isua metamorphosed sediments for early differentiation of the Earth's mantle. *Nature* 423, 428-432. https://doi.org/10.1038/nature01668

Caro, G., Bourdon, B., Birck, J-L., Moorbath, S. (2006) High-precision ^{142}Nd/^{144}Nd measurements in terrestrial rocks: Constraints on the early differentiation of the Earth's mantle. *Geochimica Cosmochimica Acta* 70, 164-191. https://doi.org/10.1016/j.gca.2005.08.015

Caro, G., Morino, P., Mojzsis, S. J., Cates, N. L., Bleeker, W. (2017) Sluggish Hadean geodynamics: Evidence from coupled ^{146,147}Sm–^{142,143}Nd systematics in Eoarchean supracrustal rocks of the Inukjuak domain (Québec). *Earth. And Planetary Science Letters* 457, 23-37. https://doi.org/10.1016/j.epsl.2016.09.051

Debaille, E., Brandon, A.D., Yin, Q.Z., Jacobsen, B. (2007) Coupled ^{142}Nd-^{143}Nd evidence for a protracted magma ocean in Mars. *Nature* 450, 525-528. https://doi.org/10.1038/nature06317

Debaille, V., O'Neil, C., Brandon, A. D., Haenecour, P., Yin, Q-Z., Mattielli, N., Treiman, A.H. (2013) Stagnant-lid tectonics in early Earth revealed by ^{142}Nd variations in late Archean rocks. *Earth Planetary Science Letters* 373, 83-92. https://doi.org/10.1016/j.epsl.2013.04.016

Fyon, J.A., Cole, S. (1989) Geology of part of the Temagami greenstone belt, District of Nipissing, including relationships between lithological, alteration, and structural features and precious-metal occurrences. In: *Summary of field work and other activities 1989*, Ontario Geological Survey Miscellaneous Paper 146, 108–115.

Li, C.-F., Wang, X.-C., Wilde, S.A., Li, X.-H., Wang, Y.-F., Li, Z. (2017) Differentiation of the early silicate Earth as recorded by ^{142}Nd-^{143}Nd in 3.8–3.0 Ga rocks from the Anshan Complex, North China Craton. *Precambrian Research* 301, 86-101. https://doi.org/10.1016/j.precamres.2017.09.001

Li, C.-F., Wang, X.-C., Li, Y.-L., Chu, Z.-Y., Guo, J.-H., Li, X.-H. (2015) Ce-Nd separation by solid-phase micro-extraction and its application to high-precision ^{142}Nd/^{144}Nd measurements using TIMS in geological materials. *Journal of Analytical Atomic Spectrometry* 30, 895-902. https://doi.org/10.1039/C4JA00328D

Maya, J.M., Bhutani, R., Balakrishnan, S., Sandhya, S.R. (2017) Petrogenesis of 3.15 Ga old Banasandra komatiites from the Dharwar craton, India: Implications for early mantle heterogeneity. *Geoscience Frontiers* 8, 467-481. https://doi.org/10.1016/j.gsf.2016.03.007

Morino, P., Caro, G., Reisburg,L., Schumacher, A. (2017) Chemical stratification in the post-magma ocean Earth inferred from coupled ^{146,147}Sm–^{142,143}Nd systematics in ultramafic rocks of the Saglek block (3.25–3.9 Ga; northern Labrador, Canada). *Earth Planetary Science Letters* 463, 136-150. https://doi.org/10.1016/j.epsl.2017.01.044

Mundl-Petermeier, A., Viehmann, S., Tusch, J., Bau, M., Kurzweil, F., Münker, C. (2022) Earth's geodynamic evolution constrained by 182W in Archean seawater. *Nature Communications* 13, 2701. https://doi.org/10.1038/s41467-022-30423-3

O'Neil, J., Carlson R.W. (2017) Building Archean cratons from Hadean mafic crust. *Science* 355, 1199-1202. https://doi.org/10.1126/science.aah3823

O'Neil, J., Carlson, R.W., Franics, D., Stevenson, R.K. (2008) Neodymium-142 Evidence for Hadean Mafic Crust. *Science* 321, 1828-1831. https://doi.org/10.1126/science.1161925

O'Neil, J., Carlson, R.W., Paquette, J-L., Francis, D. (2012) Formation age and metamorphic history of the Nuvvuagittuq Greenstone Belt. *Precambrian Res*earch 220-221, 23-44. https://doi.org/10.1016/j.precamres.2012.07.009

O'Neil, J., Rizo, H., Boyet, M., Carlson, R.W., Rosing, M.T. (2016) Geochemistry and Nd isotopic characteristics of Earth's Hadean mantle and primitive crust. *Earth Planetary Science Lett*ers 442, 194-205. https://doi.org/10.1016/j.epsl.2016.02.055

Puchtel, I.S., Blichert-Toft, J., Touboul, M., Walker, R.J., Byerly, G.R., Nisbet, E.G., Anhaeusser, C.R. (2013) Insights into early Earth from Barberton komatiites: Evidence from lithophile isotope and trace element systematics. *Geochimica. Cosmochimica Acta* 108, 63-90. https://doi.org/10.1016/j.gca.2013.01.016

Puchtel, I.S., Blichert-Toft, J., Touboul, M., Horan, M.F., Walker, R.J. (2016) The coupled ^{182}W-^{142}Nd record of early terrestrial mantle differentiation. *Geochemistry Geophysics Geosys*tems 17, 2168-2193. https://doi.org/10.1002/2016GC006324

Puchtel, I.S., Blichert-Toft, J., Touboul, M., Walker, R.J. (2018) 182W and HSE constraints from 2.7 Ga komatiites on the heterogeneous nature of the Archean mantle. *Geochimica et Cosmochimica Acta* 228, 1-26. https://doi.org/10.1016/j.gca.2018.02.030

Rizo, H., Boyet, M., Blichert-Toft, J., Rosing, M. (2011) Combined Nd and Hf isotope evidence for deep-seated source of Isua lavas. *Earth Planetary Science Letters* 312, 267-279. https://doi.org/10.1016/j.epsl.2011.10.014

Rizo, H., Boyet, M., Blichert-Toft, J., O'Niel, J., Rosing M. T., Paquette, J-L. (2012) The elusive Hadean enriched reservoir revealed by142Nd deficits in Isua Archaean rocks. *Nature* 491, 96-100. https://doi.org/10.1038/nature11565

Roth, A.S.G., Bourdon, B., Mojzsis, S.J., Rudge, J.F., Guitreau, M., Blichert‐Toft, J. (2014) Combined ^{147,146}Sm-^{143,142}Nd constraints on the longevity and residence time of early terrestrial crust. *Geochemistry, Geophysics, Geosystems* 15, 2329–2345. https://doi.org/10.1002/2014GC005313

Saji, N.S., Wielandt, D., Paton, C., Bizzarro, M. (2016) Ultra-high-precision Nd-isotope measurements of geological materials by MC-ICPMS. *Journal Analytical Atomic Spectrom*etry 31, 1490-1504. https://doi.org/10.1039/C6JA00064A

Schneider, K.P., Hoffman, J.E., Boyet, M., Münker, C., Kröner, A. (2018) Coexistence of enriched and modern-like ^{142}Nd signatures in Archean igneous rocks of the eastern Kaapvaal Craton, southern Africa. *Earth Planetary Science Letters* 487, 54-66. https://doi.org/10.1016/j.epsl.2018.01.022

Viehmann, S., Hoffmann, J.E., Münker, C., Bau, M. (2014) Decoupled Hf-Nd isotopes in Neoarchean seawater reveal weathering of emerged continents. *Geology* 42, 115–118. https://doi.org/10.1130/G35014.1

Wainwright, A.N., El Atrassi, F., Debaille, V., Mattielli, N. (2019) Geochemistry and petrogenesis of Archean mafic rocks from the Amsaga area, West African craton, Mauritania. *Precambrian Research 324*, 208-219. https://doi.org/10.1016/j.precamres.2019.02.005